PALEOBIOLOGY | Paleontological
A PUBLICATION OF THE | SOCIETY

Article

Blood flow rates to leg bones of extinct birds indicate high levels of cursorial locomotion

Qiaohui Hu* (iD), *Case Vincent Miller** (iD), *Edward P. Snelling* (iD), *and Roger S. Seymour* (iD)

Abstract.—Foramina of bones are beginning to yield more information about metabolic rates and activity levels of living and extinct species. This study investigates the relationship between estimated blood flow rate to the femur and body mass among cursorial birds extending back to the Late Cretaceous. Data from fossil foramina are compared with those of extant species, revealing similar scaling relationships for all cursorial birds and supporting crown bird–like terrestrial locomotor activity. Because the perfusion rate in long bones of birds is related to the metabolic cost of microfracture repair due to stresses applied during locomotion, as it is in mammals, this study estimates absolute blood flow rates from sizes of nutrient foramina located on the femur shafts. After differences in body mass and locomotor behaviors are accounted for, femoral bone blood flow rates in extinct species are similar to those of extant cursorial birds. Femoral robustness is generally greater in aquatic flightless birds than in terrestrial flightless and ground-dwelling flighted birds, suggesting that the morphology is shaped by life-history demands. Femoral robustness also increases in larger cursorial bird taxa, probably associated with their weight redistribution following evolutionary loss of the tail, which purportedly constrains femur length, aligns it more horizontally, and necessitates increased robustness in larger species.

Qiaohui Hu and Roger S. Seymour. School of Biological Sciences, University of Adelaide, Adelaide, SA 5005, Australia. E-mail: qiaohui.hu@adelaide.edu.au, roger.seymour@adelaide.edu.au

Case Vincent Miller. Department of Earth Sciences, The University of Hong Kong, Pok Fu Lam, Hong Kong. E-mail: Case.Miller@connect.hku.hk

Edward P. Snelling. Department of Anatomy and Physiology, and Centre for Veterinary Wildlife Research, Faculty of Veterinary Science, University of Pretoria, Pretoria, Onderstepoort 0110, South Africa. E-mail: edward.snelling@up.ac.za

Introduction

Inferring physiological functions of extinct vertebrates relies heavily on fossil bones, as not many other tissues fossilize. Fossil bones can indicate the size and weight of the animal (Campione and Evans 2020), and bone features such as bone architectural patterns can provide abundant information on functional morphology and animal behavior (Hutchinson and Allen 2009; Bishop et al. 2018). A recent method, the "foramen technique," can estimate regional blood flow by observing foramina on bone samples. This technique estimates bone perfusion rate by simply measuring bone foramen size, so it can be used with fossil bone

of extinct species. In general, the energy requirements of regional tissues determine the blood flow rates to those tissues (Wolff 2008). In particular, long bones require perfusion for bone remodeling that repairs microfractures due to stresses of locomotion and weight bearing (Lieberman et al. 2003; Robling et al. 2006; Eriksen 2010). The intensity of bone metabolic demand, and hence blood flow rate, is affected by loading and exercise (Sim and Kelly 1970; Rubin and Lanyon 1984; Beverly et al. 1989). Blood flow rates in turn determine the sizes of the arteries (Seymour et al. 2019b). Where arteries pass through bone, the size of the foramen can be used to evaluate blood flow rate, thus a larger foramen indicates a higher blood flow

0094-8373/23

rate and implies a higher metabolic rate. The foramen technique was first used to relate nutrient foramen sizes on femoral bones to locomotor activity levels of living mammals and non-avian reptiles in comparison with Cretaceous dinosaurs (Seymour et al. 2012). Since then, additional studies have used this technique to investigate the relationships among foramen size, regional blood flow rate, and local tissue metabolism (Allan et al. 2014; Seymour et al. 2015, 2016; Boyer and Harrington 2018, 2019; Hu et al. 2018, 2021a,b; Newham et al. 2020; Knaus et al. 2021).

The foramen technique provides an opportunity to investigate extinct animals' blood flow rates without preservation of blood vessels. Moreover, estimated blood flow rates can be associated with extinct animals' metabolic rates, lifestyles, and habitats. This technique has been used to investigate metabolic rates in fossil archosauriform sauropsids (reptile relatives) and synapsids (mammal relatives). Both groups had femoral nutrient foramina of similar or larger size than those of living mammals, revealing that they had high femoral bone perfusion and consequently were likely very active animals (Seymour et al. 2012, 2019a; Knaus et al. 2021). This is consistent with growing evidence that amniotes evolved high metabolic rates before the split into sauropsids and synapsids (Grigg et al. 2022). Allan et al. (2014) studied the nutrient foramina of living birds and recently extinct New Zealand moa, finding blood flow to femoral bone was significantly higher in primarily cursorial species than in volant species, in line with greater locomotory reliance on the legs of cursors. Allan's study also suggests that the blood flow was approximately two times higher in bipedal cursorial birds than in quadrupedal mammals, further supporting the theory that blood flow to the femora is related to locomotory stresses and bone microfracture repair (Lieberman et al. 2003; Robling et al. 2006). Apart from locomotor activities, femoral bone perfusion has also been related to other physiological processes, including bone growth and calcium mobilization. For example, femoral nutrient foramen areas tend to be relatively larger in young, growing kangaroos than in adults (Hu et al. 2018), probably due to a higher energy demand for bone growth. Femoral bone blood flow in laying domestic fowl is higher than in subadult non-laying hens (Hu et al. 2021a), possibly associated with calcium mobilization for eggshell production and provisioning the yolk for embryonic skeleton growth.

Whether long-extinct (>1000 years) cursorial birds have the same locomotor intensity as living species remains unresolved, because their femoral bone blood flows have not been studied and compared. Although birds exhibit a wide range of locomotor behaviors, this study focuses only on those species that are always or usually flightless. It examines the femora of ground-dwelling and aquatic birds, including living and extinct species, to investigate the scaling relationships of femoral bone blood flow rates on body masses. We use improved approaches to evaluate blood flow from nutrient foramen size. The previous approach (Allen et al. 2014) involved calculating the "blood flow index," Q_i, which assumed that the nutrient arterial radius was proportional to foramen radius and that flow rate was proportional to the artery radius cubed, according to Poiseuille-Hagen theory (Pfitzner 1976). The arbitrary units of Q_i (mm^3) were initially useful for comparative purposes, but the proportionality between the artery and foramen size was not known, and the theoretical and empirical relationships between absolute blood flow rate and arterial radius are now known to be inconsistent with Poiseuille flow (Huo and Kassab 2016; Seymour et al. 2019b). This study is an improvement over the blood flow index method and represents a further improvement to the foramen technique by considering both the proportion of the foramen area occupied by the nutrient artery (Hu et al. 2021a) and using an empirical relationship between absolute blood flow rate ($\dot{Q}$; ml s^{-1}) and arterial radius (Seymour et al. 2019b).

Birds are commonly accepted to have evolved from theropod dinosaurs (Ostrom 1973, 1976; Padian and Chiappe 1998; Pittman et al. 2020). Throughout the evolution of Theropoda, one common trait change on the evolutionary line to birds is the femora changing orientation from a nearly vertical to a nearly horizontal position (Gatesy 1990; Gatesy and

Biewener 1991; Hutchinson and Allen 2009). Such change results in shorter but more robust femora compared with non-avian theropods, which keeps the knee in line with the center of gravity and compensates for higher torsional stains applied to femora (Gatesy 1990; Gatesy and Biewener 1991; Carrano 1998). Femur circumference is expected to increase at a faster rate than femur length as birds increase in body mass (Chan 2017), thereby increasing bone robustness (Janis et al. 2014). Because the sizes of weight-bearing bones are related to body mass, this study measures femur lengths and midshaft circumferences of the cursorial birds to compare estimated femur blood perfusion rate with the size of the bone.

Materials and Methods

Specimens.—In total, 154 femora (74 pairs, and 6 singles) from 28 living cursorial bird species and 45 femora (5 pairs, and 35 singles) from 21 extinct species (between the Late Cretaceous and Quaternary) were analyzed from collections at the South Australian Museum and the Smithsonian National Museum of Natural History. We use the term "cursorial birds" to describe those that cannot fly (terrestrial flightless birds) or those that can fly but use walking and running as their primary mode of locomotion (ground-dwelling flighted birds). Some aquatic flightless birds, such as penguins (Sphenisciformes), *Hesperornis*, and *Baptornis*, also are included. Specimen and species details are summarized in Table A1.

Measurements and Calculations.—Femur length (L; mm) and midshaft circumference (C; mm) were measured to 1 mm with a ruler and measuring tape. For very small femora, the midshaft circumference was instead calculated, assuming an ellipse-shaped cross section and measuring two orthogonal diameters with a set of calipers. Robustness (R) was calculated as C/L. Following now established methods (Hu et al. 2020), photos of foramen openings located along the central one-third of the femur were classified as nutrient foramina and captured with a scale (set alongside and in the same plane as the opening) using a digital microscope camera connected to a computer running image acquisition software

(AMCap v. 9.016). Foramina located more distally along the femur were excluded as being metaphyseal, epiphyseal, or pneumatic foramina. Foramen passages on all fossil bones in this study were similar to those of extant species and were apparently unchanged by diagenesis and were often filled with contrasting matrix. Best-fit ellipses of the foramen openings were determined using the Fiji image processing package,[1] and the foramen dimensions, including major and minor diameters (mm) and foramen area (mm^2), were recorded (Fig. 1).

A nutrient foramen is generally occupied by both a nutrient artery and a vein. Studies on chickens indicate that the lumen of the artery occupies approximately 20% of the total nutrient foramen area (Hu et al. 2021a), allowing us to estimate the inner radius of the artery from foramen area. Arterial inner radii cannot be directly estimated from a multiple-foramen femur, as the nutrient artery and vein arrangement can vary from a foramen occupied by an artery only, a vein only, or a pair of vessels. However, paired femora with one and two foramina each have similar summed foramen areas (Hu et al. 2021a), and the total bone blood flow rates between the left and right femora are also not significantly different (Hu et al. 2021b). Therefore, the absolute femoral bone blood flow of a multiple-foramen femur can be calculated by treating the summed foramen area as if it were the area of a single foramen. Following an approach validated on chickens (Hu et al. 2021a), where multiple nutrient foramina were present in a femur, the areas of all foramina were summed, and arterial inner radius was calculated from the total. Given arterial inner radius, the blood flow rate could be estimated according to equation (1). In this empirical equation, derived from 50 in vivo studies of mammals (Seymour et al. 2019b), absolute arterial blood flow rate ($\dot{Q}$; ml s^{-1}) is related to arterial lumen radius (r_i; mm):

$$\log \dot{Q} = -0.20 (\log r_i)^2 + 2.31 \log r_i - 0.29 \quad (1)$$
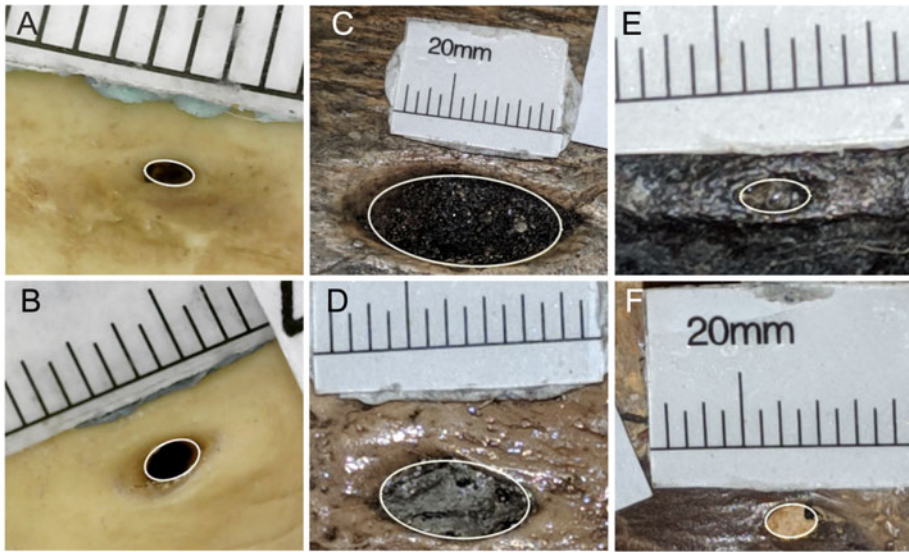
[1]Open Source, www.fiji.sc.

FIGURE 1. Exemplary scaled images of femoral foramen openings captured from (A) living Australian bustard (*Ardeotis australis*), (B) living emu (*Dromaius novaehollandiae*), (C) recently extinct elephant bird (*Aepyornis* sp.), (D) recently extinct bush moa (*Anomalopteryx fortis*), (E) extinct Eocene *Lithornis promiscuus*, and (F) extinct Late Cretaceous aquatic *Hesperornis regalis*. Best-fit ellipses of the foramen external openings were determined using the Fiji image processing package. The smallest scale increment is 0.5 mm.

This equation indicates that flow rate is not proportional to radius raised to the exponent 3 as predicted by theoretical laminar flow rates in ideal tubes according to a Poiseuille flow regime. Instead, the relationship is curved, varying between an exponent of 2 in the largest arteries to 3 in capillaries. Unfortunately, a dedicated equation for birds is unavailable due to lack of data. However, paired measurements for $\dot{Q}$ (0.011 ml s^{-1}) and r_i (0.23 mm) in the carotid artery of budgerigars (*Melopsittacus undulatus*) (Schmaier et al. 2011), are within the 95% confidence limits around a $\dot{Q}$ of 0.014 ml s^{-1} predicted from equation (1) when r_i is 0.23 mm. Femur shaft blood flow rates of domestic chickens measured using fluorescent microspheres are not significantly different from the blood flow rates estimated using equation (1) from the radii of nutrient arteries filled with contrast media and CT scanned (Hu et al. 2021a,b). Even if the relationship between flow rate and arterial size is not identical in birds and mammals, we use the same equation for all species in our study, so any differences will be conserved.

In bird specimens having both femora, the data for L, C, and $\dot{Q}$ were averaged; otherwise,

values for the single available femur are presented. Data from multiple individuals of the same species were averaged to obtain single values used in statistics for each species. For comparison, femoral bone blood flow index (Q_i) was also calculated as $Q_i = r_i^4/L$, according to the previous studies (Seymour et al. 2012; Allan et al. 2014).

Statistical Analyses.—Mean values for $\dot{Q}$, L, C, and R were analyzed in relation to body mass (M_b; g) and locomotor behavior. Differences in the scaling of $\dot{Q}$ on M_b between living and extinct cursorial birds (i.e., slope and intercept) were assessed by subjecting the log-transformed relationships to analysis of covariance (Zar 1998) using statistical software (Prism v. 6.0, GraphPad Software, La Jolla, CA, USA). The software also calculated and applied 95% confidence interval bands onto the scaling relationships and identified potential outliers. For comparison, Q_i on M_b was also plotted and compared with $\dot{Q}$ on M_b. The relationship of C and L was investigated for all cursorial birds. A measurement of L in *Genyornis newtoni* was not possible, so only foramen area, C, and $\dot{Q}$ of this species were included in the analyses. An estimate of M_b of

all cursorial birds was made by averaging the values calculated from two equations based on femur circumferences, C (Campbell and Marcus 1992: table 2; Dickison 2007: table 3.5). Juvenile specimens were excluded, because their nutrient foramen areas tend to be relatively larger, presumably due to the extra perfusion requirements for growth (Hu et al. 2018). To identify likely juvenile specimens, M_b values for adult living cursorial bird species taken from the literature (del Hoyo et al. 1992; Higgins et al. 2006; https://animaldiversity.org; http://datazone.birdlife.org) were compared with those values estimated from C and subsequently excluded from the interspecific scaling analyses if the mean circumference-based value was less than 50% of the literature value. The same approach could not be used for fossil specimens, so instead we selected relatively larger fossil femora for extinct species for which multiple fossils were available. Sample sizes of between 1 and 13 (average of 2.4) were obtained for each of the living and extinct cursorial bird species (Table A1). Five living species had no adult individuals measured; therefore, these juvenile specimens were excluded from all scaling relationship analyses. However, their femur foramen and morphological data were included for comparisons of right and left femora. M_b was calculated from measurements of C for each species and was used for specific M_b-related analyses. However, the scaling of C on M_b in living cursorial bird species involved only M_b values collected from the literature to achieve independence between these two variables.

If a specimen had one femur with one nutrient foramen and the other femur with multiple foramina, the summed foramen areas were compared between these femur pairs using a paired t-test. Most extinct species had only one femur preserved. To test how accurately one femur can represent the morphological values for a missing femur, the nutrient foramen area, L, and C were compared between left and right femora of all femur pairs in living species, including immature samples, again using a paired t-test. We also divided the bird species into three different groups (terrestrial flightless, ground-dwelling flighted birds, and aquatic flightless species) (Table A1) to investigate whether different locomotor behaviors can

influence $\dot{Q}$ and R. We hypothesized that the terrestrial flightless birds have a higher blood flow rate than the other two groups.

Results

Effect of Body Mass on Femoral Blood Flow Rate.—Across all cursorial bird species analyzed in this study, the estimated body masses (M_b) of the extinct species range from 615 g to 565 kg, which represents a 918-fold range, and the M_b values of the living species range from 27 g to 148 kg, which represents a 5562-fold range (Table A1). The estimated single femoral bone blood flow rate ($\dot{Q}$) varies from 4.22×10^{-5} to 0.36 ml s^{-1} across both the living and extinct species. The relationship between blood flow rate and body mass is allometric. The foramen datum from the ostrich (*Struthio camelus*) was identified as an outlier and excluded from the blood flow and foramen analyses. $\dot{Q}$ scales with M_b to the 0.74 ± 0.20 power in living species and to the 0.87 ± 0.23 power in extinct species (Fig. 2A). There are no significant differences in either the scaling exponents ($F_{1, 39} = 0.76$; $p = 0.39$) or scaling elevations ($F_{1, 40} = 1.08$; $p = 0.31$) between the living and extinct species. If all birds, except for the ostrich, are considered as a whole dataset, the scaling relationship is $\dot{Q} = 3.69 \times 10^{-6} M_b^{0.85 \pm 0.10}$ (Fig. 2B). If we use Q_i instead of $\dot{Q}$ to represent femoral blood flow, Q_i of all cursorial birds in this study scales with M_b to the 1.04 ± 0.16 power (Fig. 2C).

We obtained original data on foramen size and published body masses of 15 living cursorial birds species reported by Allan et al. (2014) and calculated $\dot{Q}$, instead of the original blood flow index Q_i, resulting in the equation $\dot{Q} = 9.33 \times 10^{-6} M_b^{0.61 \pm 0.22}$. The scaling exponent and elevation are not significantly different from our living cursorial birds (scaling exponents, $F_{1, 34} = 0.11$; $p = 0.74$; scaling elevations, $F_{1, 35} = 0.81$; $p = 0.38$).

Left and Right Nutrient Foramen Dimensions and Femur Morphology.—For those specimens with a single foramen in one femur and multiple foramina in the opposing femur, a paired t-test indicates that the area of the single foramen is not significantly different from the summed area of the multiple foramina ($p =$
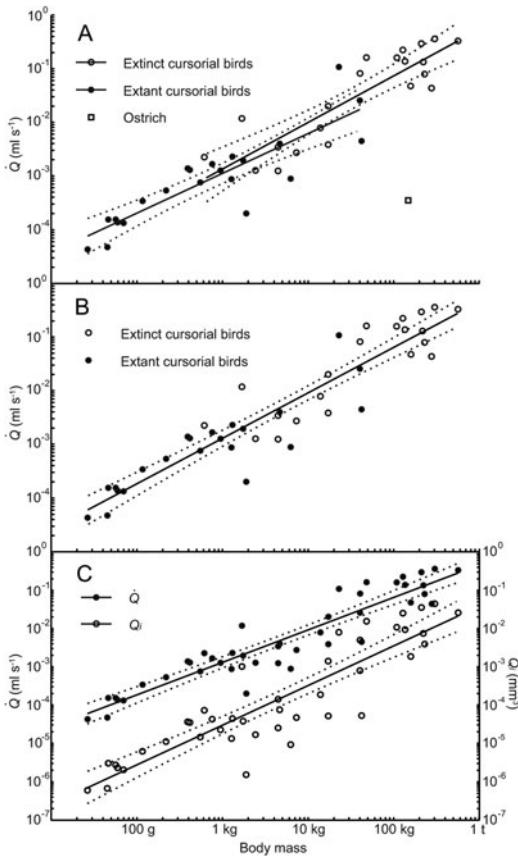
FIGURE 2. Relationships among femoral bone blood flow rate ($\dot{Q}$; ml s^{-1}), femoral bone blood flow index (Q_i, mm^3), and body mass (M_b; g) in living and extinct adult cursorial birds. A, The scaling equations are: $\dot{Q} = 6.58 \times 10^{-6}\ M_b^{0.74\ \pm\ 0.20}$ for 22 living species and $\dot{Q} = 3.34 \times 10^{-6}\ M_b^{0.87\ \pm\ 0.23}$ for 21 extinct species. The single outlier for the ostrich (*Struthio camelus*) is not included in the regressions. B, Living and extinct species ($n = 43$) are combined, and the overall scaling equation is $\dot{Q} = 3.69 \times 10^{-6}\ M_b^{0.85\ \pm\ 0.10}$. C, The scaling equation of Q_i among 42 living and extinct cursorial birds species ($Q_i = 2.30 \times 10^{-8}\ M_b^{1.04\ \pm\ 0.16}$) compared with scaling of $\dot{Q}$ indicated in B. Q_i of *Genyornis newtoni* is not included due to unknown femur length. The dotted lines demarcate the 95% confidence intervals for each regression mean. The units of $\dot{Q}$ and Q_i are different; therefore, only the exponents (line slopes) can be compared.

0.16; $N = 18$ femur pairs). Similarly, left and right femora of living species do not differ significantly in total foramen area ($p = 0.67$, $N = 83$ femur pairs), femur length (L) ($p = 0.28$, $N = 84$ femur pairs) or midshaft circumference (C) ($p = 0.14$, $N = 84$ femur pairs).

Effect of Body Mass on Femur Morphology.—Across all cursorial birds, L scales with M_b according to the relationship $L = 10.21 M_b^{0.28\ \pm\ 0.02}$. When M_b is calculated from C according to
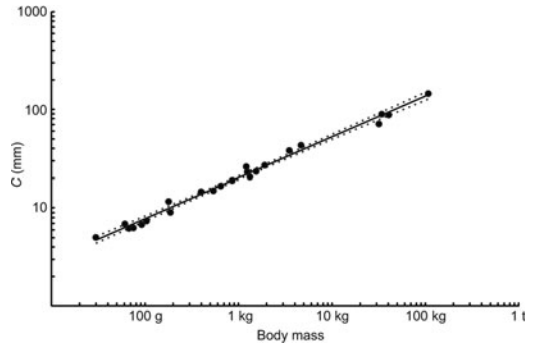

FIGURE 3. Relationships between femur cross-sectional circumference (C; mm) and literature body-mass (M_b; g) values in 23 living adult cursorial bird species. The allometric equation is $C = 1.15 M_b^{0.42\ \pm\ 0.02}$. The dotted lines are 95% confidence intervals for the regression mean.

previous studies (Campbell and Marcus 1992; Dickison 2007), the resulting allometric equation is $C = 1.43 M_b^{0.39}$, with no residual error. If we instead use literature values of M_b for living species, the equation is only slightly steeper, $C = 1.15 M_b^{0.42\ \pm\ 0.02}$ ($R^2 = 0.99$) (Fig. 3). Across all birds, C scales with L as $C = 0.081 L^{1.32\ \pm\ 0.10}$ ($R^2 = 0.94$), and robustness (R) scales with M_b as $R = 0.14 M_b^{0.11\ \pm\ 0.02}$ ($R^2 = 0.72$).

Effect of Body Mass and Locomotor Behavior on Femoral Blood Flow Rate and Femur Morphology.—The scaling of $\dot{Q}$ on M_b among the three groups with different locomotor behaviors (terrestrial flightless, ground-dwelling flighted, and aquatic flightless birds) has neither significantly different scaling exponents ($F_{2,\ 37} = 1.16$, $p = 0.32$) nor significantly different scaling elevations ($F_{2,\ 39} = 0.79$, $p = 0.46$). Scaling equations for R on M_b among the three locomotor behavior groups are: $R = 0.08 M_b^{0.15\ \pm\ 0.04}$ (terrestrial flightless birds), $R = 0.20 M_b^{0.12\ \pm\ 1.30}$ (aquatic flighted birds), and $R = 0.15 M_b^{0.10\ \pm\ 0.04}$ (ground-dwelling flighted birds). Neither the scaling exponents ($F_{1,\ 35} = 3.74$, $p = 0.06$) nor the scaling elevations ($F_{1,\ 36} = 1.11$, $p = 0.30$) of R on M_b are significantly different between the terrestrial flightless and ground-dwelling flighted birds. Aquatic flightless birds, however, have a higher scaling elevation than the other two groups combined ($F_{1,\ 40} = 33.61$, $p < 0.001$) (Fig. 4). Importantly, aquatic flightless birds in this study cover a very narrow range of M_b, so the allometric exponent is not significant.
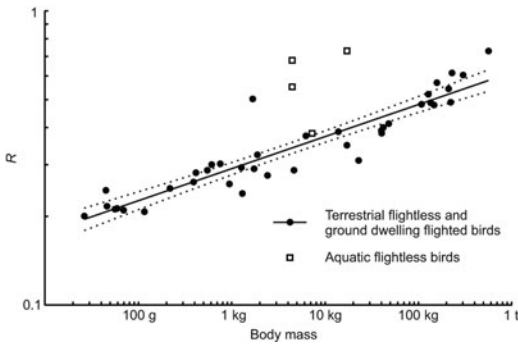
FIGURE 4. Relationship between femoral robustness ($R = C/L$) and body mass (M_b; g) in living and extinct terrestrial flightless, ground-dwelling flighted, and aquatic flightless adult birds. Terrestrial flightless species ($n = 18$) and ground-dwelling flighted species ($n = 21$) are combined and described by the relationship $R = 0.14 M_b^{0.11 \pm 0.01}$. Data for aquatic flightless species ($n = 4$) are plotted separately. The dotted lines are 95% confidence intervals for the regression means.

Discussion

Effect of Body Mass on Femoral Blood Flow Rate.—Scaling of $\dot{Q}$ on M_b is statistically indistinguishable between living and extinct cursorial birds (Fig. 2A,B). The combined dataset of 43 species, including the small ground-dwelling but flighted birds and larger flightless runners, extends the body-size range to three orders of magnitude and results in the overall allometric equation $\dot{Q} = 3.69 \times 10^{-6} M_b^{0.85 \pm 0.10}$. The exponent of 0.85 falls within the 95% confidence interval range of the scaling exponents of the maximum aerobic metabolic rate during treadmill locomotion in mammals (0.87 ± 0.05) (White and Seymour 2005; Seymour et al. 2012) and birds (1.02 ± 0.22) (Allan et al. 2014). This indicates that femoral blood flow rate is associated with the intensity of terrestrial locomotion among adult cursorial birds, assuming that the maximum aerobic energy produced during locomotion is related to the stresses placed on the bones that result in microfractures requiring repair. Our earlier study of living birds revealed the connection between locomotory stresses on bones and bone perfusion; both blood flow index and femur mass were approximately two times higher in primarily cursorial species than in primarily volant species (Allan et al. 2014). In other words, species that more regularly put

greater forces on their legs have thicker femora and greater bone perfusion. Among cursorial species, femur bone mass was related to $M_b^{1.16}$ (Allan et al. 2014). Here we show that femur $\dot{Q}$ is related to $M_b^{0.85}$; therefore, $\dot{Q}$ is proportional to femur mass raised to the 0.73 power (= 0.85/1.16). Unfortunately, we could not measure original bone mass in fossil species to compare with living species, but the $\dot{Q}$ values in extinct species are unremarkable.

The very low $\dot{Q}$ of the ostrich is notable as an outlier and consequently was removed from the analysis. Of the two ostriches included in this study, one individual had a femur with one tiny midshaft nutrient foramen, and the other individual had a femur with no foramen at all. We have not encountered anything like this in a decade of study of femoral nutrient foramina, and we have no definite explanation for it. The other two large ratites, the southern cassowary (*Casuarius casuarius*) and emu (*Dromaius novaehollandiae*), have high femoral blood flow values expected of large, active cursors. The pattern of bone vascular anatomy may be inherently different in the ostrich.

The scaling of $\dot{Q}$ produces less variance in the regression than that for Q_i and therefore appears to be an improvement on the Q_i concept (Fig. 2C). As expected, the scaling exponent for $\dot{Q}$ is less than that for Q_i, because $\dot{Q}$ is derived from a polynomial equation with an effective exponent less than 3, whereas Q_i depends on radius raised to the power of 3. We thus recommend $\dot{Q}$ over Q_i in future estimations of animal blood flow.

Nutrient Foramen and Femur Morphology.—If one femur of a bird has one nutrient foramen and the other has more than one, the summed areas of both are not significantly different ($N = 18$), which agrees with the previous findings in chickens (Hu et al. 2021a). Foramen area ($p = 0.67$), L ($p = 0.28$), and C ($p = 0.14$) are not significantly different between the left and right femora of 84 femur pairs in living species. Therefore, one femur can well represent the femur morphological data of the animal in general, in agreement with other studies of fossils (Hedrick et al. 2019). In some cases, we found that areas can be very different between both femora. In 9 of the 84 femur pairs available for comparison, foramen area was two to

seven times larger in one femur than in the opposing femur, revealing potential error when analyzing a single femur, especially in extinct birds that typically had only one femur preserved. Therefore, although one femur can well represent the femur morphological data of the animal in general, we still recommend measuring foramen areas of both femora when possible.

Across all birds in this study, L scales with M_b to the power of 0.28 ± 0.02, which is not significantly different from 0.30 ± 0.03 or 0.306 reported in flightless birds by Doube et al. (2012) and Cubo and Casinos (1996), respectively. The scaling of C on M_b in all cursorial birds has an exponent of 0.39. The exponent is slightly shallower than the exponent of C on M_b in our sample of living cursorial bird collected from the literature (0.42 ± 0.02) (Fig. 3). The exponent of 0.42 ± 0.02 is not significantly different from the exponents of 0.40 ± 0.05 reported for running birds (Maloiy et al. 1979), 0.41 ± 0.02 for 75 bird species with no classified locomotor status (Anderson et al. 1985), and 0.43 ± 0.02 for the midshaft diameter in flightless birds (Cubo and Casinos 1996). Leg bone midshaft circumferences are strongly related to animal body mass (Campione and Evans 2012). Theoretically, any length scales with body mass raised to the 0.33 power if body shape is geometrically proportional. All exponents for C in birds are not only significantly higher than 0.33, but also significantly higher than 0.35 ± 0.02 or 0.35 ± 0.01 found in mammals (Anderson et al. 1985; Campione and Evans 2012). Thus, the exponent difference is substantial between mammals and birds. In mammals, there is a transition from crouched postures to more upright postures as body mass increases (as well as reduced locomotor performance in very large species), purportedly to maintain similar peak bone stresses (Alexander et al. 1979; Biewener 1989). Similar to mammals, the whole legs of larger cursorial birds tend to be more upright than those of smaller species (Gatesy and Biewener 1991; Birn-Jeffery et al. 2014; Daley and Birn-Jeffery 2018). However, how the orientation of the femur alone changes with body size across cursorial bird species is unknown. It is hypothesized that bird femora evolved a horizontal orientation to compensate for the shift in center of gravity due to tail reduction (Gatesy 1990; Gatesy and Biewener 1991; Hutchinson and Allen 2009). The relatively lower post-acetabular body mass of birds compared with the long-tailed theropods leads to a more anterior center of gravity, which constrains L in birds (Gatesy 1991; Christiansen and Bonde 2002). C increases at a faster rate than L across all cursorial birds (1.32 ± 0.10), which agrees with previous studies (Gatesy 1991; Gatesy and Biewener 1991; Chan 2017). R increases with body mass with a scaling exponent of 0.11 ± 0.02, which is significantly steeper than 0. The relatively robust femora in larger birds may be required to maintain the crouched posture with increasing body mass.

The scaling of $\dot{Q}$ on M_b is similar among the three locomotor groups, with exponents and elevations not significantly different from one another. The scaling of R on M_b in aquatic flightless birds, however, has a higher scaling elevation than the other two groups (Fig. 4). The change in femur proportion across different taxa may have little impact on femoral bone blood flow. The higher robustness in the aquatic flightless birds may be explained by their locomotor behaviors differing from those of terrestrial birds. Because the aquatic flightless birds in this study include just four species across a narrow body-mass range, no definitive conclusions can be drawn. Our aquatic flightless category also contains both wing-propelled and foot-propelled swimmers, whose locomotion greatly differs mechanically but could not be examined separately due to the small sample size. Future studies with a wider range of body mass and aquatic locomotor behavior are required to draw a solid conclusion as to whether $\dot{Q}$ is indeed not significantly different between the aquatic birds and terrestrial cursorial birds. Our terrestrial categories similarly do not differentiate more and less cursorial taxa. Larger sample sizes of each may reveal variation not captured in this study. At the current resolution, the scaling of $\dot{Q}$ on M_b is also not significantly different between the ground-dwelling flighted and terrestrial flightless birds, revealing that the femoral blood flow rate alone may not be enough to distinguish locomotor behaviors in cursorial birds,

especially when they all have similar primary modes of locomotion (i.e., in this case, walking and running).

Conclusions

In summary, absolute femoral bone blood flow can be estimated for both living and extinct cursorial birds from the size of the nutrient foramen. The absolute flow rates reveal a tighter relationship to body mass than bone blood flow index values reported in previous studies. A single equation for scaling of femoral bone blood flow on body mass ($\dot{Q} = 3.69 \times 10^{-6}$ $M_b^{0.85 \pm 0.10}$) can be applied to both living and extinct cursorial birds. Femoral bone shaft perfusion appears to be strongly affected by femoral mass, which scales with body mass with a hyperallometric exponent in cursorial species. Femur midshaft circumference increases more steeply with body mass in cursorial birds than in mammals. Femur midshaft circumference increases faster than length in cursorial birds as body mass increases, and robustness tends to increase in larger cursorial birds. This is likely because of their proportionally greater preacetabular body mass restricting femur length, and the horizontal orientation of the femur necessitating thicker femora to compensate for greater torsional loading. Different locomotor behaviors among the cursorial birds do not strongly affect their femoral bone blood flow scaling, but they do have an impact on the scaling of robustness.

Acknowledgments

Declaration of Competing Interests

The authors declare no competing interests.

Literature Cited

Alexander, R. M., G. Maloiy, B. Hunter, A. Jayes, and J. Nturibi. 1979. Mechanical stresses in fast locomotion of buffalo (*Syncews coffer*) and elephant (*Loxodonta africana*). Journal of Zoology 189:135–144.

Allan, G. H., P. Cassey, E. P. Snelling, S. K. Maloney, and R. S. Seymour. 2014. Blood flow for bone remodelling correlates with locomotion in living and extinct birds. Journal of Experimental Biology 217:2956–2962.

Anderson, J. F., A. Hall-Martin, and D. A. Russell. 1985. Long-bone circumference and weight in mammals, birds and dinosaurs. Journal of Zoology 207:53–61.

Beverly, M. C., T. A. Rider, M. J. Evans, and R. Smith. 1989. Local bone mineral response to brief exercise that stresses the skeleton. British Medical Journal 299:233–235.

Biewener, A. A. 1989. Scaling body support in mammals: limb posture and muscle mechanics. Science 245:45–48.

Birn-Jeffery, A. V., C. M. Hubicki, Y. Blum, D. Renjewski, J. W. Hurst, and M. A. Daley. 2014. Don't break a leg: running birds from quail to ostrich prioritise leg safety and economy on uneven terrain. Journal of Experimental Biology 217:3786–3796.

Bishop, P. J., S. A. Hocknull, C. J. Clemente, J. R. Hutchinson, A. A. Farke, R. S. Barrett, and D. G. Lloyd. 2018. Cancellous bone and theropod dinosaur locomotion. Part III—Inferring posture and locomotor biomechanics in extinct theropods, and its evolution on the line to birds. PeerJ 6:e5777.

Boyer, D. M., and A. R. Harrington. 2018. Scaling of bony canals for encephalic vessels in euarchontans: implications for the role of the vertebral artery and brain metabolism. Journal of Human Evolution 114:85–101.

Boyer, D. M., and A. R. Harrington. 2019. New estimates of blood flow rates in the vertebral artery of euarchontans and their implications for encephalic blood flow scaling: a response to Seymour and Snelling (2018). Journal of Human Evolution 128:93–98.

Campbell, K. E., and L. Marcus. 1992. The relationship of hindlimb bone dimensions to body weight in birds. Natural History Museum of Los Angeles County Science Series 36:395–412.

Campione, N. E., and D. C. Evans. 2012. A universal scaling relationship between body mass and proximal limb bone dimensions in quadrupedal terrestrial tetrapods. BMC Biology 10:1–22.

Campione, N. E., and D. C. Evans. 2020. The accuracy and precision of body mass estimation in non-avian dinosaurs. Biological Reviews 95:1759–1797.

Carrano, M. T. 1998. Locomotion in non-avian dinosaurs: integrating data from hindlimb kinematics, in vivo strains, and bone morphology. Paleobiology 24:450–469.

Chan, N. R. 2017. Phylogenetic variation in hind-limb bone scaling of flightless theropods. Paleobiology 43:129–143.

Christiansen, P., and N. Bonde. 2002. Limb proportions and avian terrestrial locomotion. Journal für Ornithologie 143:356–371.

Cubo, J., and A. Casinos. 1996. Flightlessness and long bone allometry in Palaeognathiformes and Sphenisciformes. Netherlands Journal of Zoology 47:209–226.

Daley, M. A., and A. Birn-Jeffery. 2018. Scaling of avian bipedal locomotion reveals independent effects of body mass and leg posture on gait. Journal of Experimental Biology 221:jeb152538.

del Hoyo, J., A. Elliott, and J. Sargatal. 1992. Handbook of the birds of the world. Lynx Edicions, Barcelona.

Dickison, M. R. 2007. The allometry of giant flightless birds. PhD thesis. Duke University, Durham, N.C.

Doube, M., S. C. Yen, M. M. Kłosowski, A. A. Farke, J. R. Hutchinson, and S. J. Shefelbine. 2012. Whole-bone scaling of the avian pelvic limb. Journal of Anatomy 221:21–29.

Eriksen, E. F. 2010. Cellular mechanisms of bone remodeling. Reviews in Endocrine and Metabolic Disorders 11:219–227.

Gatesy, S. M. 1990. Caudofemoral musculature and the evolution of theropod locomotion. Paleobiology 16:170–186.

Gatesy, S. M. 1991. Hind limb scaling in birds and other theropods: implications for terrestrial locomotion. Journal of Morphology 209:83–96.

Gatesy, S. M, and A. A. Biewener. 1991. Bipedal locomotion: effects of speed, size and limb posture in birds and humans. Journal of Zoology 224:127–147.

Grigg, G., J. Nowack, J. E. P. W. Bicudo, N. C. Bal, H. N. Woodward, and R. S. Seymour. 2022. Whole-body endothermy: ancient, homologous and widespread among the ancestors of mammals, birds and crocodylians. Biological Reviews 97:766–801.

Hedrick, B. P., E. R. Schachner, G. Rivera, P. Dodson, and S. E. Pierce. 2019. The effects of skeletal asymmetry on interpreting biologic variation and taphonomy in the fossil record. Paleobiology 45:154–166.

Higgins, P., J. Peter, S. Cowling, W. Steele, and S. Davies. 2006. Handbook of Australian, New Zealand and Antarctic birds. Oxford University Press, Melbourne.

Hu, Q., T. J. Nelson, E. P. Snelling, and R. S. Seymour. 2018. Femoral bone perfusion through the nutrient foramen during growth and locomotor development of western grey kangaroos (*Macropus fuliginosus*). Journal of Experimental Biology 221:1–6.

Hu, Q., T. J. Nelson, and R. S. Seymour. 2020. Bone foramen dimensions and blood flow calculation: best practices. Journal of Anatomy 236:357–369.

Hu, Q., T. J. Nelson, and R. S. Seymour. 2021a. Morphology of the nutrient artery and its foramen in relation to femoral bone perfusion rates of laying and non-laying hens. Journal of Anatomy 240:94–106.

Hu, Q., T. J. Nelson, and R. S. Seymour. 2021b. Regional femoral bone blood flow rates in laying and non-laying chickens estimated with fluorescent microspheres. Journal of Experimental Biology 224:jeb242597.

Huo, Y., and G. S. Kassab. 2016. Scaling laws of coronary circulation in health and disease. Journal of Biomechanics 49:2531–2539.

Hutchinson, J. R., and V. Allen. 2009. The evolutionary continuum of limb function from early theropods to birds. Naturwissenschaften 96:423–448.

Janis, C. M., K. Buttrill, and B. Figueirido. 2014. Locomotion in extinct giant kangaroos: were sthenurines hop-less monsters? PLoS ONE 9:e109888.

Knaus, P. L., A. H. Van Heteren, J. K. Lungmus, and P. M. Sander. 2021. Higher blood flow into the femur indicates elevated aerobic capacity in synapsids since the reptile-mammal split. Frontiers in Ecology and Evolution 9:751238.

Lieberman, D. E., O. M. Pearson, J. D. Polk, B. Demes, and A. W. Crompton. 2003. Optimization of bone growth and remodeling in response to loading in tapered mammalian limbs. Journal of Experimental Biology 206:3125–3138.

Maloiy, G., R. M. Alexander, R. Njau, and A. Jayes. 1979. Allometry of the legs of running birds. Journal of Zoology 187:161–167.

Newham, E., P. G. Gill, P. Brewer, M. J. Benton, V. Fernandez, N. J. Gostling, D. Haberthür, J. Jernvall, T. Kankaanpää, and A. Kallonen. 2020. Reptile-like physiology in Early Jurassic stem-mammals. Nature Communications 11:1–13.

Ostrom, J. H. 1973. The ancestry of birds. Nature 242:136–136.

Ostrom, J. H. 1976. *Archaeopteryx* and the origin of birds. Biological Journal of the Linnean Society 8:91–182.

Padian, K., and L. M. Chiappe. 1998. The origin of birds and their flight. Scientific American 278:38–47.

Pfitzner, J. 1976. Poiseuille and his law. Anaesthesia 31:273–275.

Pittman, M., J. O'Connor, D. J. Field, A. H. Turner, W. Ma, P. Makovicky, and X. Xu. 2020. Pennaraptoran systematics. Pp. 7–36 *in* M. Pittman and X. Xu, eds. Pennaraptoran theropod dinosaurs: past progress and new frontiers. Bulletin of American Museum of Natural History Library, New York.

Robling, A. G., A. B. Castillo, and C. H. Turner. 2006. Biomechanical and molecular regulation of bone remodeling. Annual Review of Biomedical Engineering 8:455–498.

Rubin, C. T., and L. E. Lanyon. 1984. Regulation of bone formation by applied dynamic loads. Journal of Bone and Joint Surgery 66:397–402.

Schmaier, A. A., T. J. Stalker, J. J. Runge, D. Lee, C. Nagaswami, P. Mericko, M. Chen, S. Cliché, C. Gariépy, and L. F. Brass. 2011. Occlusive thrombi arise in mammals but not birds in response to arterial injury: evolutionary insight into human cardiovascular disease. Blood, the Journal of the American Society of Hematology 118:3661–3669.

Seymour, R. S., S. L. Smith, C. R. White, D. M. Henderson, and D. Schwarz-Wings. 2012. Blood flow to long bones indicates activity metabolism in mammals, reptiles and dinosaurs. Proceedings of the Royal Society of London B 279:451–456.

Seymour, R. S., S. E. Angove, E. P. Snelling, and P. Cassey. 2015. Scaling of cerebral blood perfusion in primates and marsupials. Journal of Experimental Biology 218:2631–2640.

Seymour, R. S., V. Bosiocic, and E. P. Snelling. 2016. Fossil skulls reveal that blood flow rate to the brain increased faster than brain volume during human evolution. Royal Society Open Science 3:160305.

Seymour, R. S., M. Ezcurra, D. Henderson, M. E. Jones, S. C. Maidment, C. V. Miller, S. J. Nesbitt, D. Schwarz, C. Sullivan, and E. Wilberg. 2019a. Large nutrient foramina in fossil femora indicate intense locomotor and metabolic activity in Triassic archosauromorphs and the pseudosuchian lineage. Society for Vertebrate Paleontology meeting, Abstracts, p. 190.

Seymour, R. S., Q. Hu, E. P. Snelling, and C. R. White. 2019b. Interspecific scaling of blood flow rates and arterial sizes in mammals. Journal of Experimental Biology 222:jeb199554.

Sim, F. H., and P. J. Kelly. 1970. Relationship of bone remodeling, oxygen consumption, and blood flow in bone. Journal of Bone and Joint Surgery 52:1377–1389.

White, C. R., and R. S. Seymour. 2005. Allometric scaling of mammalian metabolism. Journal of Experimental Biology 208:1611–1619.

Wolff, C. B. 2008. Normal cardiac output, oxygen delivery and oxygen extraction. Advances in Experimental Medicine and Biology 599:169–182.

Zar, J. H. 1998. Biostatistical analysis. Prentice-Hall, Englewood Cliffs, N.J.

Appendix

TABLE A1. Femur and femoral nutrient foramen size values and femoral bone blood flow rates ($\dot{Q}$) of 28 living and 21 extinct cursorial birds collected from Smithsonian National Museum of Natural History (SNMNH) and South Australian Museum (SAM). Each species was classified with different locomotor behaviors. Asterisks (*) indicate species excluded from the scaling relationship analyses because they were immature animals. However, their data were included while comparing femur morphologies and foramen sizes between both femora.

Species	Replicates	Femur length (mm)	Femur circumference (mm)	Estimated body mass (g)	Literature body mass (g)	Foramen area (mm²)	$\dot{Q}$ (ml s⁻¹)	Q_i (mm³)	Groups	Museum
Living cursorial birds										
Acryllium vulturinum	1	81	21	947	1330	0.13	1.26×10^{-3}	2.22×10^{-5}	Flighted	SAM
*Aptenodytes patagonicus**	1	90	36	3743	12,150	0.049	3.16×10^{-4}	2.68×10^{-6}	Aquatic flightless	SAM
Apteryx owenii	2	79	23	1269	1243	0.10	8.73×10^{-4}	1.32×10^{-5}	Terrestrial flightless	SAM
Ardeotis australis	4	115	43	6241	4683	0.10	8.82×10^{-4}	9.19×10^{-6}	Flighted	SAM
Burhinus grallarius	3	58	17	551	648	0.091	7.54×10^{-4}	1.45×10^{-5}	Flighted	SAM
Callipepla californica	1	44	9	116	188	0.051	3.40×10^{-4}	6.14×10^{-6}	Flighted	SAM
Casuarius casuarius	5	226	88	40,084	40,600	1.33	2.58×10^{-2}	7.88×10^{-4}	Terrestrial flightless	SAM
Coturnix pectoralis	2	35	7	70	105	0.026	1.32×10^{-4}	2.01×10^{-6}	Flighted	SAM
Dromaius novaehollandiae	13	225	90	41,901	34,233	0.34	4.47×10^{-3}	5.24×10^{-5}	Terrestrial flightless	SAM
*Eudyptes chrysocome**	1	74	27	1768	2715	0.14	1.35×10^{-3}	2.66×10^{-5}	Aquatic flightless	SAM
*Eudyptes pachyrhynchus**	5	72	24	1439	3820	0.083	6.65×10^{-4}	9.81×10^{-6}	Aquatic flightless	SAM
*Eudyptula minor**	4	51	16	454	1467	0.043	2.67×10^{-4}	3.76×10^{-6}	Aquatic flightless	SAM
Fulica atra	4	53	15	416	540	0.13	1.29×10^{-3}	3.46×10^{-5}	Flighted	SAM
Gallirallus philippensis	4	47	12	219	180	0.071	5.32×10^{-4}	1.09×10^{-5}	Flighted	SAM
Leipoa ocellata	5	84	27	1886	1917	0.035	1.98×10^{-4}	1.49×10^{-6}	Flighted	SAM
Meleagris gallopavo	2	133	38	4649	3525	0.31	3.99×10^{-3}	7.44×10^{-5}	Flighted	SAM
Nestor notabilis	1	63	19	757	862	0.16	1.67×10^{-3}	4.27×10^{-5}	Flighted	SAM
Pedionomus torquatus	1	25	6	45	68	0.013	4.65×10^{-5}	6.61×10^{-7}	Flighted	SAM
Pezoporus wallicus	1	29	6	46	75	0.029	1.53×10^{-4}	2.99×10^{-6}	Flighted	SAM
Phasianus colchicus	1	91	26	1735	1214	0.18	1.95×10^{-3}	3.75×10^{-5}	Flighted	SAM
Porzana fluminea	4	32	7	59	61	0.027	1.36×10^{-4}	2.26×10^{-6}	Flighted	SAM
Rhea americana	1	231	72	22,882	32,000	4.23	1.09×10^{-1}	7.87×10^{-3}	Terrestrial flightless	SAM
Struthio camelus	2	305	146	147,681	107,500	0.052	3.48×10^{-4}	9.11×10^{-7}	Terrestrial flightless	SAM
Tragopan sp.	2	98	24	1301	1550	0.21	2.30×10^{-3}	4.41×10^{-5}	Flighted	SAM
Tribonyx ventralis	3	56	15	393	400	0.14	1.38×10^{-4}	3.63×10^{-5}	Flighted	SAM
Turnix varius	4	32	7	56	92.5	0.029	1.53×10^{-4}	2.71×10^{-6}	Flighted	SAM
Zapornia pusilla	2	25	5	27	30	0.012	4.22×10^{-5}	5.83×10^{-7}	Flighted	SAM
*Zapornia tabuensis**	1	30	6	41	45	0.016	6.36×10^{-5}	8.49×10^{-7}	Flighted	SAM
Extinct cursorial birds										
Aepyornis hildebrandti	1	280	172	228,459	N/A	3.29	7.99×10^{-2}	3.91×10^{-3}	Terrestrial flightless	SAM
Aepyornis maximus	1	332	242	564,520	N/A	10.82	3.33×10^{-1}	2.57×10^{-2}	Terrestrial flightless	SNMNH
Aepyornis sp.	1	316	191	301,386	N/A	11.71	3.64×10^{-1}	4.39×10^{-2}	Terrestrial flightless	SNMNH
Anomalopteryx didiformis	1	230	95	48,188	N/A	5.92	1.63×10^{-1}	1.55×10^{-2}	Terrestrial flightless	SNMNH

Anthropornis nordenskjoeldi	1	120	46	7296	N/A	0.24	2.73×10^{-3}	4.66×10^{-5}	Aquatic flightless	SNMNH
Baptornis advenus	1	69	38	4459	N/A	0.13	1.24×10^{-3}	2.52×10^{-5}	Aquatic flightless	SNMNH
Dinornis novaezealandiae	3	264	150	163,358	N/A	2.73	6.66×10^{-2}	3.86×10^{-3}	Terrestrial flightless	SNMNH and SAM
Dinornis robustus	1	290	141	135,270	N/A	5.16	1.38×10^{-1}	9.29×10^{-3}	Terrestrial flightless	SAM
Emeus crassus	9	269	129	108,933	N/A	6.58	1.89×10^{-1}	1.36×10^{-2}	Terrestrial flightless	SNMNH and SAM
Euryapteryx gravis	3	265	138	128,299	N/A	7.70	2.25×10^{-1}	2.52×10^{-2}	Terrestrial flightless	SAM
Gastornis sp.	1	348	170	221,509	N/A	5.03	1.34×10^{-1}	7.36×10^{-3}	Terrestrial flightless	SNMNH
Genyornis newtoni	1	N/A	185	276,981	N/A	2.02	4.38×10^{-2}	N/A	Terrestrial flightless	SAM
Hesperornis regalis	1	88	64	17,154	N/A	1.09	2.02×10^{-2}	1.39×10^{-3}	Aquatic flightless	SNMNH
Hesperornis sp.	1	56	38	4459	N/A	0.28	3.43×10^{-3}	1.41×10^{-4}	Aquatic flightless	SNMNH
Lithornis plebius	1	58	18	615	N/A	0.20	2.25×10^{-3}	7.30×10^{-5}	Flighted	SNMNH
Lithornis promiscuus	1	52	26	1684	N/A	0.72	1.18×10^{-2}	1.01×10^{-3}	Flighted	SNMNH
Megalapteryx didinus	1	232	89	40,482	N/A	3.36	8.19×10^{-2}	4.92×10^{-3}	Terrestrial flightless	SNMNH and SAM
Pachyornis elephantopus	8	307	167	210,768	N/A	10.86	3.40×10^{-1}	4.62×10^{-2}	Terrestrial flightless	SNMNH and SAM
Paracathartes howardae	1	109	30	2430	N/A	0.13	1.26×10^{-3}	1.65×10^{-5}	Flighted	SNMNH
Pezophaps solitaria	1	184	64	17,154	N/A	0.31	3.86×10^{-3}	5.15×10^{-5}	Terrestrial flightless	SNMNH
Raphus cucullatus	1	152	59	13,890	N/A	0.53	7.92×10^{-3}	1.85×10^{-4}	Terrestrial flightless	SNMNH